Pupil alignment considerations for large, deployable space telescopes

Brent J. Bos*, Raymond G. Ohl and David A. Kubalak
NASA Goddard Space Flight Center, Mail Code 551, Greenbelt, MD, USA 20771

ABSTRACT

For many optical systems the properties and alignment of the internal apertures and pupils are not critical or controlled with high precision during optical system design, fabrication or assembly. In wide angle imaging systems, for instance, the entrance pupil position and orientation is typically unconstrained and varies over the system's field of view in order to optimize image quality. Aperture tolerances usually do not receive the same amount of scrutiny as optical surface aberrations or throughput characteristics because performance degradation is typically graceful with misalignment, generally only causing a slight reduction in system sensitivity due to vignetting. But for a large deployable space-based observatory like the James Webb Space Telescope (JWST), we have found that pupil alignment is a key parameter. For in addition to vignetting, JWST pupil errors cause uncertainty in the wavefront sensing process that is used to construct the observatory on-orbit. Furthermore they also open stray light paths that degrade the science return from some of the telescope's instrument channels. In response to these consequences, we have developed several pupil measurement techniques for the cryogenic vacuum test where JWST science instrument pupil alignment is verified. These approaches use pupil alignment references within the JWST science instruments; pupil imaging lenses in three science instrument channels; and unique pupil characterization features in the optical test equipment. This will allow us to verify and crosscheck the lateral pupil alignment of the JWST science instruments to approximately 1-2% of their pupil diameters.

Keywords: James Webb Space Telescope, pupil alignment, space telescope, optical alignment, optics

1. INTRODUCTION

In an optical system, pupils exist wherever images, real or virtual, of the system's internal aperture stop are formed. Two key pupil images of interest are the entrance pupil and the exit pupil. The entrance pupil is the image of the aperture stop as viewed from object space. The exit pupil is the image of the aperture stop as viewed from image space. Pupil characterization and internal aperture stop alignment in many optical systems are typically not considered to be key or driving performance considerations. During the design optimization process, pupil image characteristics are often allowed to be free variables so that the available degrees of freedom can be used to maintain magnification, improve image quality and control distortion. For instance, in wide angle imaging systems the entrance pupil position, shape and orientation are often left to vary significantly over the system's field of view while maintaining image quality. Aperture and pupil tolerances usually do not receive the same amount of scrutiny as optical surface aberrations or throughput characteristics because the performance degradation is typically graceful with misalignment, generally only causing a slight reduction in system sensitivity due to vignetting. But our work developing the James Webb Space Telescope (JWST)[1] has revealed that pupil alignment, characterization and calibration are key parameters that impact JWST performance. Since JWST is potentially the first of the next generation of large, deployable space telescopes, we expect the pupil alignment and pupil quality to be important to the success of those future observatories as well. Given the diameters of current launch vehicle fairings, and those expected to be available in the near future, some amount of on-orbit assembly will be required. This will create pupil alignment considerations that are similar to JWST's. The on-orbit assembly will also necessitate some type of image quality assessment, similar to the JWST wavefront sensing and control process.

JWST is a 6 m-class, space-based, infrared observatory designed to study the formation and evolution of stars and galaxies in the early Universe approximately 200 million years after it began (see Figure 1). The observatory will be launched into an orbit about the second Lagrange point of the earth-sun system, approximately 1.5 million km away

*Brent.J.Bos@nasa.gov; phone 1 301 286-5670

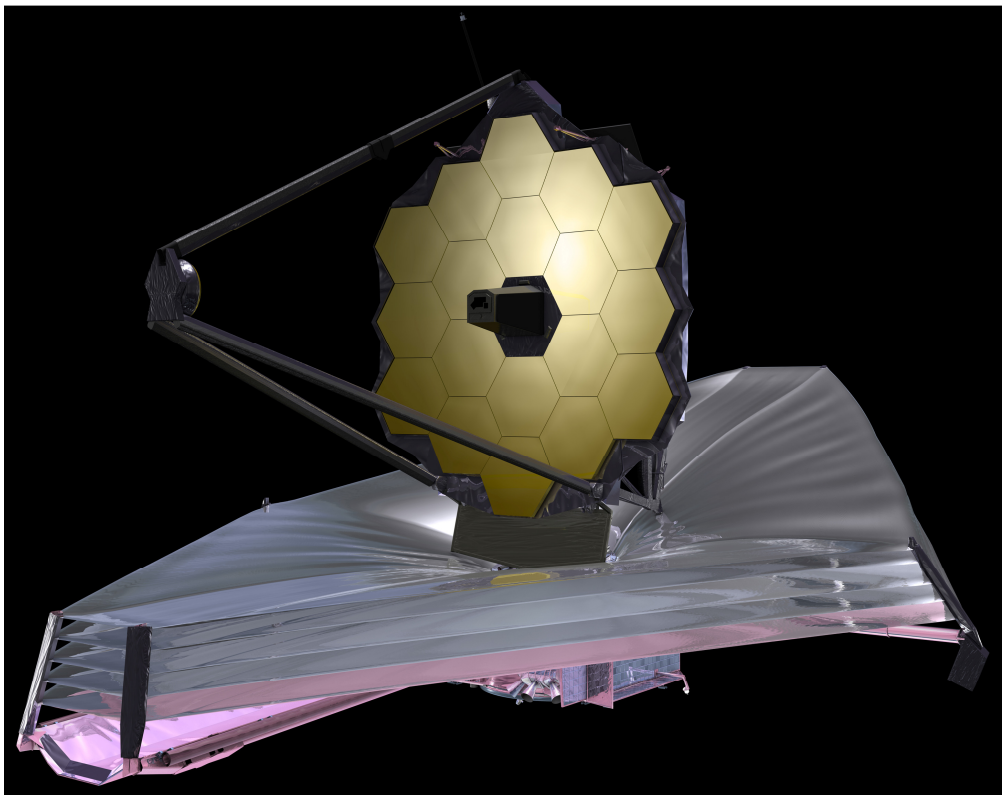

Figure 1. Artist's rendition of the James Webb Space Telescope. The 18 individual mirror segments that make up the telescope's primary mirror are clearly visible as is the aft-optics sub-assembly (AOS) aperture at the center of the primary mirror.

from the earth, and passively cooled to 30-50 K to facilitate astronomical observations in the 0.6 to 28 μm wavelength band.

The JWST observatory consists of three primary elements: the spacecraft, the Optical Telescope Element (OTE) and the Integrated Science Instrument Module (ISIM). The major spacecraft elements consist of an attitude control system, the spacecraft electronics and the observatory sunshield. In terms of physical size, the sunshield is the single largest observatory subsystem and is designed to keep the OTE and ISIM in perpetual shade to passively cool those elements down to their cryogenic operating temperatures.

The observatory's telescope mirrors are the primary components of the OTE. The optical prescription is based upon an on-axis, three-mirror, anastigmat design form and includes a flat, fine steering mirror (FSM) located near the telescope exit pupil to compensate for low frequency image motion – bringing the total number of monolithic OTE mirror surfaces to four. The low areal density primary mirror (~15 kg/m^2) is a segmented aperture constructed from 18 hexagonal segments. The mirror segments are folded and stowed prior to launch to enable the observatory to fit within an Ariane 5 launch vehicle. After launch, the primary mirror segments are deployed and optically phased using mechanical actuators and wavefront sensing algorithms to produce diffraction-limited performance at approximately 2 μm.

The ISIM Element primarily consists of a mechanical metering structure (the ISIM structure), three science instruments and a fine guidance sensor with significant scientific capability. The ISIM structure is a composite tube truss structure designed and built by the NASA Goddard Space Flight Center with industrial partner ATK[1]. The University of Arizona is providing a near-infrared camera (NIRCam) which also contains the primary wavefront sensing hardware for the observatory[2]. A near-infrared, multi-object spectrograph (NIRSpec) is being provided by the European Space Agency[3] and a European consortium teamed with the Jet Propulsion Laboratory is providing a mid-infrared instrument (MIRI)[4]. Rounding out the ISIM instrument complement is a fine guidance sensor (FGS-Guider) from the Canadian Space Agency[5] which also contains an imaging channel with a versatile near-infrared filtering capability (FGS-TFI), a recent

modification from the original etalon filtering approach that was originally baselined[6]. The basic ISIM optical design layout and arrangement of the science instruments within the ISIM structure is described by Bos et al[7].

2. KEY JWST PUPIL ALIGNMENT CONSIDERATIONS

2.1 Vignetting

In order to see the birth of the first stars and galaxies in the Universe, JWST is designed to be extremely sensitive to the red-shifted light coming from those objects, providing signal-to-noise ratio images of 10 or better with 10^{-34} W/m^2/Hz sensitivity at 2 μm and slightly better than 10^{-32} W/m^2/Hz sensitivity at 10 μm. The observatory's primary mirror aperture, detector quantum efficiencies and optical throughput have been designed and specified to meet those levels at the end of the mission's life.

Those sensitivity performance levels will be degraded if the light collected by the JWST primary mirror, the aperture stop in the system, is clipped by any of the apertures in the optical telescope element (OTE) or the science instruments. This is called vignetting. If the beam clipping occurs at an aperture that is not close to a pupil, then the vignetting is rather benign and sensitivity is only lost near the edges of an instrument's field of view. But vignetting that is caused by a surface that is located close to or at a pupil image has a more severe impact on system performance. Beam clipping that occurs at a pupil located inside a science instrument reduces sensitivity across the instrument's entire field of view. Beam clipping caused by a telescope aperture located at a pupil has an even more profound impact on observatory performance. Vignetting that occurs there reduces sensitivity across the entire telescope's field of view and in turn uniformly degrades the sensitivity of every science instrument in the observatory.

A common approach for mitigating vignetting risks in large observatories is to oversize the optical apertures such that some misalignment between the various apertures can occur and not cause the loss of any light. But the amount of over sizing possible is usually limited by one or more factors: mass, volume or system geometry (particularly for folded reflective systems). In addition, oftentimes a system's optical designer will fail to appreciate the adjustability, alignment complexities and tolerances of their system, causing them to be overly optimistic in the nominal specification of their optics' clear apertures. It is typically this oversight that causes vignetting at the edges of instruments' fields of view. On JWST the apertures have typically been oversized by approximately 5% wherever possible to reduce the likelihood of any vignetting.

2.2 Coronagagraphy

Three of the JWST science instruments (NIRCam, MIRI and FGS-TFI) have coronagraphic imaging modes, primarily to facilitate the discovery and observation of extra-solar planets and disks. Pupil misalignments are typically more detrimental to coronagraphic observations than they are to standard imaging. The shape and dimensions of the Lyot stops used in coronagraphs are designed to be a compromise between optical throughput and the suppression of diffraction artifacts in the planes of the instrument detectors. If the Lyot stop does not allow enough light to pass through the system, then even with highly effective diffraction suppression the photon or instrument detector noise will render impossible the observation of the dim objects of interest. If on the other hand the Lyot stop does not block enough light, then the diffraction features caused by the bright object located close to the objects of interest will saturate the scene and also render the objects of interest unobservable. To achieve the maximum coronagraphic imaging performance possible from a system with an aperture of a given size, perfect alignment between the coronagraph's stop and the system's aperture stop and other pupil obscurations is required. The three JWST instrument coronagraph channels have been designed with different estimates for pupil alignment error since perfect alignment is unlikely to be achieved. The total observatory-level pupil alignment error is estimated not to exceed 3.8% of the pupil diameters and so each of the Lyot stops have been constructed with that value as one of the key design drivers.

2.3 Wavefront sensing

JWST is too large to be launched into space fully constructed and so its final assembly will occur in space after launch and separation from the final stage of its Ariane 5 launch vehicle. The on-orbit optical alignment process will be monitored and guided using a series of processes called wavefront sensing. One of the key wavefront sensing steps is to use phase retrieval to do the final optimization of the observatory's optical alignment. Phase retrieval relies on knowledge of the system's exit pupil amplitude function to generate accurate estimates for the system's wavefront error. Although algorithms and techniques can be used to simultaneously recover pupil amplitude and phase when pupil amplitude information is unavailable, the algorithm phase estimates are not as accurate as when pupil amplitude is well

understood. Routines that recover both amplitude and phase are better used as crosschecks on the available pupil information.

Performance evaluations of the JWST phase retrieval algorithm indicate that knowledge of two pupil amplitude characteristics are particularly important for achieving the required wavefront measurement accuracy: exit pupil distortion and amplitude variability. Exit pupil distortion knowledge is important because it is used to construct the overall shape of the as-built JWST exit pupil which is used as the assumed starting point for the phase retrieval pupil amplitude function. Amplitude variability is the change in optical throughput across the JWST pupil caused by optical coatings, pupil aberrations and the vignetting described in Section 2.1.

2.4 Stray light

The fourth and final pupil alignment issue that we have identified as being important to the performance of JWST is related to stray light suppression. Due to the open architecture of the JWST optical design (i.e., no tube or baffle between the primary and secondary mirrors) and the particular three mirror anastigmat design solution chosen for the telescope's design in July 2003 when the OTE was modified from an F/17 to an F/20 design, JWST has a particularly onerous stray light path that will significantly degrade the mission's science return if it happens to be excited on-orbit. The path consists of a straight shot from a star, or other radiant object in the sky, directly to an instrument's pick-off mirror without reflecting off any of the OTE optics. The path originates from outside of the designed JWST field of view, travels just over the outer boundary of the FSM aperture mask and then strikes the instrument pick-off mirrors; injecting the stray light into the designed optical path of the instruments. This generates a curvilinear blur across the instrument detectors that cannot be calibrated out (see Figure 2). The JWST Project has dubbed this particular stray light path the "rogue path."

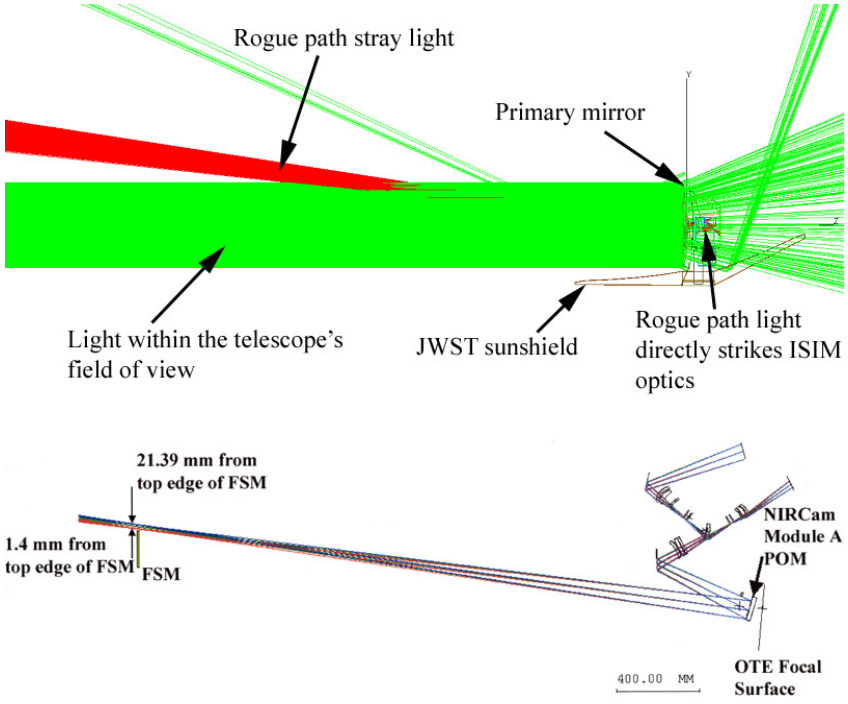

Figure 2. The top ray trace shows the nominal imaging field of view of the JWST telescope in green. The red rays show the rogue path stray light that can strike the instrument pick-off mirrors (POM) and travel all the way to the instrument detectors without reflecting off an OTE mirror. The bottom ray trace shows the physical explanation for how the rogue path stray light can enter the science instrument optics. A specific example for the NIRCam Module A channel is shown. The rogue path stray light appears to come from a slightly oversized exit pupil (the OTE exit pupil is located near the FSM) and the extra clear aperture margin that the instruments' have designed into their optical paths to guard against vignetting allows the stray light to travel through the entire optical train until it strikes a detector.

The mitigation chosen to block the JWST rogue path stray light was to create an overlap between the OTE FSM aperture mask and the internal aperture stops of the science instruments. The outer diameter of the FSM aperture mask was increased until it obscured the light traveling from the secondary mirror to the tertiary mirror as much as possible without vignetting the NIRCam fields of view. The inner diameters of the science instrument aperture stops were only made large enough to accommodate the expected pupil misalignment between the OTE and science instruments. The outer diameters of the instrument aperture stops were maximized to block light any light that might travel around the outer edge of the FSM mask. In the nominal design configuration, this aperture mask arrangement completely blocks the rogue path. The rogue path suppression only fails if lateral misalignment causes the inner aperture stop projection of the instrument's aperture at the FSM mask to fall beyond the outer perimeter of the FSM mask (see Figure 3). The mask apertures have been sized so that the rogue path is suppressed for misalignments up to approximately 6% of the nominal pupil diameter. In addition, due to the location and design of the OTE's aft-optics assembly aperture stop, the rogue path can only open up when the pupil misalignment occurs in one particular direction, providing additional margin against this significant observatory degradation.

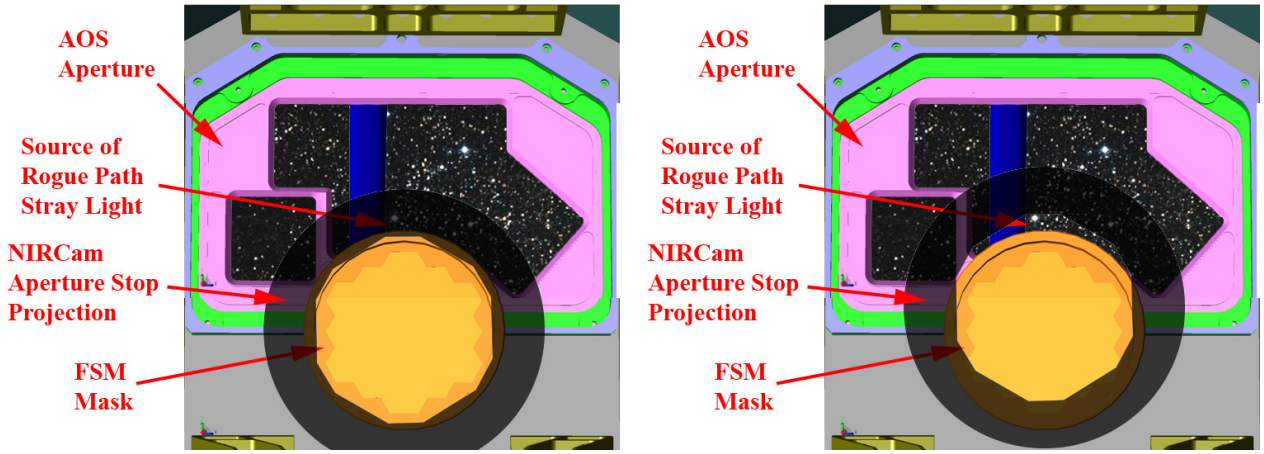

Figure 3. Illustration of how the rogue path stray light is blocked by the combination of the FSM aperture mask and the internal aperture stops of the JWST science instruments. The image on the left shows how good pupil alignment blocks the rogue path stray light from entering the science instruments. The image on the right shows how lateral pupil misalignment in the direction of the AOS aperture center opens up the rogue path – allowing star light to fall directly on the instrument pick-off mirrors (POM) without ever reflecting off an OTE mirror.

3. PUPIL VERIFICATION METHODS

3.1 Pupil verification trades

Due to the optical test architecture developed for the JWST program, the most thorough investigation of the telescope's pupil alignment will occur during the ISIM Element's cryogenic thermal vacuum test campaign using an OTE surrogate called the OSIM (OTE Simulator)[8,9]. During the observatory-level testing, currently planned to occur in the large (27 m high and 17 m diameter internal volume) thermal vacuum chamber, Chamber A, at the Johnson Space Center (JSC)[10], pupil characteristics will only be checked at three points in the telescope's field of view. So to ensure that the primary JWST pupil verification generates the data of interest, we studied and analyzed a variety of pupil test techniques for the ISIM Element test campaign. The techniques we considered fell into one of three basic architecture types: radiometric analysis at the science instrument detector planes; pupil obscurations in the OSIM and science instrument apertures; and reflective pupil alignment references located in the science instrument optical path. The primary metric we used to compare the efficacy of the various techniques was the accuracy with which we could measure the lateral pupil misalignment or pupil shear, since this is a key degree of freedom related to vignetting and suppression of the stray light rogue path. Based on the expected construction and assembly errors associated with the flight hardware and the pupil

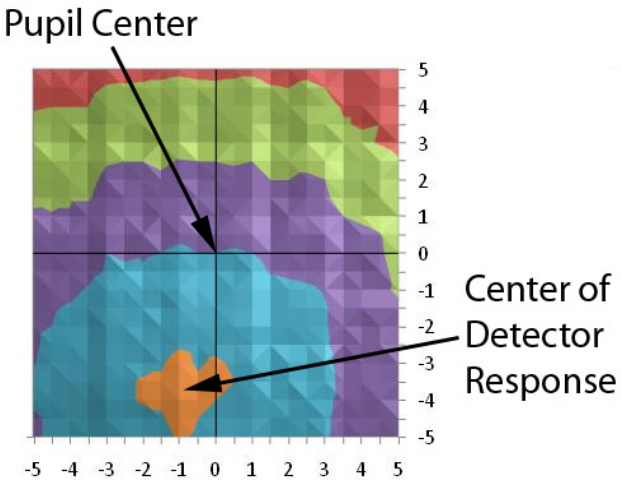

Figure 4. Example of the response predicted in the NIRCam long wavelength channel caused by laterally scanning a special OSIM aperture mask and recording the detector response as a function of mask position. Even without any detector noise modeled, the center of the detector response is not coincident with the position for perfect pupil alignment.

shear constraints described in Section 2, we required a measurement approach to verify the lateral pupil alignment to within 0.5-1% of pupil diameters.

The radiometric-based approach we considered for the ISIM Element testing was based on the idea that the total optical throughput at an instrument's detector could be monitored while an OSIM aperture mask is translated laterally until the detector's response is observed to drop by a significant amount. Several more similar scans would then be conducted in multiple directions to generate a two-dimensional instrument response versus OSIM aperture mask position function. First order optics leads you to believe that the first moment or centroid of the instrument response versus mask position would be coincident with the location of the center of a science instrument's projected entrance pupil. This approach was extremely attractive to us because, unlike the other two measurement approaches, it did not require the introduction of any special hardware into the science instruments.

We analyzed this radiometric-based approach using optical ray trace models of the JWST science instruments and the OSIM and found that the center of the science instrument's projected entrance pupils could not be reliably found using this approach, at least not to the required 1% of the pupil diameters. Different types of OSIM apertures were evaluated but still the pupil shear measurement uncertainties were several times too large compared to what was needed, even without including any detector noise in the simulation. Figure 4 shows an example of the NIRCam long wavelength response which illustrates the problem with the radiometric-based approach. Although we didn't quantitatively assess the individual contributors to this behavior, we attributed most of the problem to be due to the holes in the OSIM pupil (a consequence of the OSIM's optical design), the pupil aberrations designed into the science instruments and the shape of the instrument aperture stops and clear apertures. Although the technique was predicted to work in a coarse sense, we decided to not pursue it any further due to its lack of precision. In addition, even if the pupil shear measurement could be done with the necessary accuracy, this technique was incapable of generating pupil roll or clocking information.

The second pupil measurement approach we considered was more intrusive to the design of the science instruments than the radiometry-based approach but would take advantage of functionality already built into the OSIM design. This approach would require the introduction of special opaque features into the science instrument and OSIM pupil planes. These fiducials would then be made observable in the instrument detector planes by introducing defocus into the optical path through combined translations of the OSIM focus adjustment mechanism and the science instrument focus adjustment mechanisms. We considered the suitability of several basic geometrical shapes for pupil fiducials but expended the most analysis effort in evaluating the ability to use circularly opaque fiducials to generate near-field diffraction "Arago spots" in the instrument detector planes. Figure 5 shows an example of this at the NIRSpec detector plane.

The presence of the Arago spots in the simulated science instrument images provided excellent features for making pupil measurements and seemed promising. Unfortunately we ultimately determined that even the combined motion provided by both the OSIM and the science instrument focus adjustment mechanisms would not be able to introduce enough defocus into the system to make it possible to generate images where the opaque fiducials could be clearly identified and measured. Even with the maximum amount of defocus introduced into the system the images were predicted to more closely resemble out-of-focus point spread functions rather than pupil images with discernible features.

The primary pupil measurement approach we decided on for the ISIM Element verification campaign is one that utilizes reflective pupil alignment references located at or near pupil planes in the JWST science instruments and uses a special detector in the OSIM to measure pupil alignment. Although this approach was arguably the most invasive of the three approaches considered, requiring the introduction of special hardware into the flight science instruments and a detector system into OSIM, it was the only one of the three predicted to measure pupil shear to the required accuracy of ~1% and also provides pupil roll measurements.

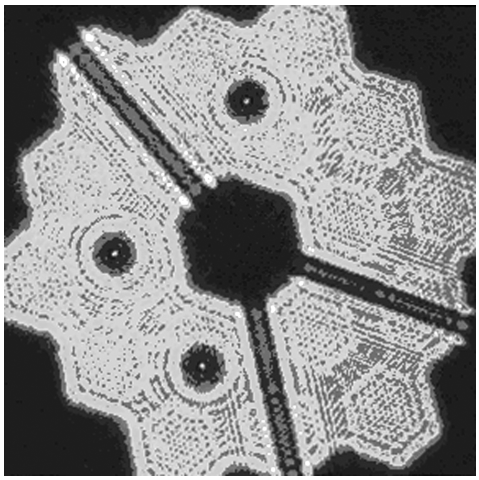

Figure 5. Diffraction simulation of three Arago spots generated in the NIRSpec detector plane by opaque circular fiducials in the instrument pupil plane. Although images of suitable quality for high accuracy pupil alignment measurements could be simulated, in practice the amount of defocus required to generate those images was beyond the capability of the JWST flight and ground support equipment hardware.

3.2 Pupil alignment reference (PAR) measurement

The baseline ISIM Element pupil verification approach using pupil alignment references (PAR) is described in detail by Bos et al[9]. The technique functions as shown in Figure 6. Light from a single field point in OSIM passes through the OSIM PAR and then reflects off of a beam splitter where it is directed into the science instrument under test. The OSIM PAR is a clear aperture with opaque fiducials that is rotated into the OSIM aperture stop position for the pupil alignment test. Once the light passes through it, the position of the OSIM aperture stop is encoded in the beam. After the light from the OSIM enters the science instrument it travels until it reflects off of the instrument PAR which is a specularly reflective mirror with opaque fiducials located at or near the science instrument's pupil plane. At that point the relative position between the OSIM PAR and the science instrument PAR is encoded in the beam. The light then travels back out of the instrument towards the OSIM, passes through the OSIM beamsplitter and then is collected by a detector in the OSIM's pupil imaging module (PIM)[8] (Figure 7 shows an image of the PIM hardware being prepared for cryogenic performance verification). The collected image is then analyzed to determine the relative location and rotation of the science instrument PAR with respect to the OSIM PAR. The OSIM PAR calibration data is used to calculate the location and rotation of the science instrument PAR in the JWST coordinate system. Finally, the positions of the science instrument pupils are determined by using science instrument calibration data that relates the position of the PAR to the actual pupils used for science observations.

The PAR measurement approach allows us to measure the three key pupil alignment degrees of freedom: lateral motion up and down, lateral motion side-to-side and rotation. The other degrees of freedom, tip/tilt and focus, can be estimated from the PAR data by measuring the image cosine effects and image scale, but not to high precision.

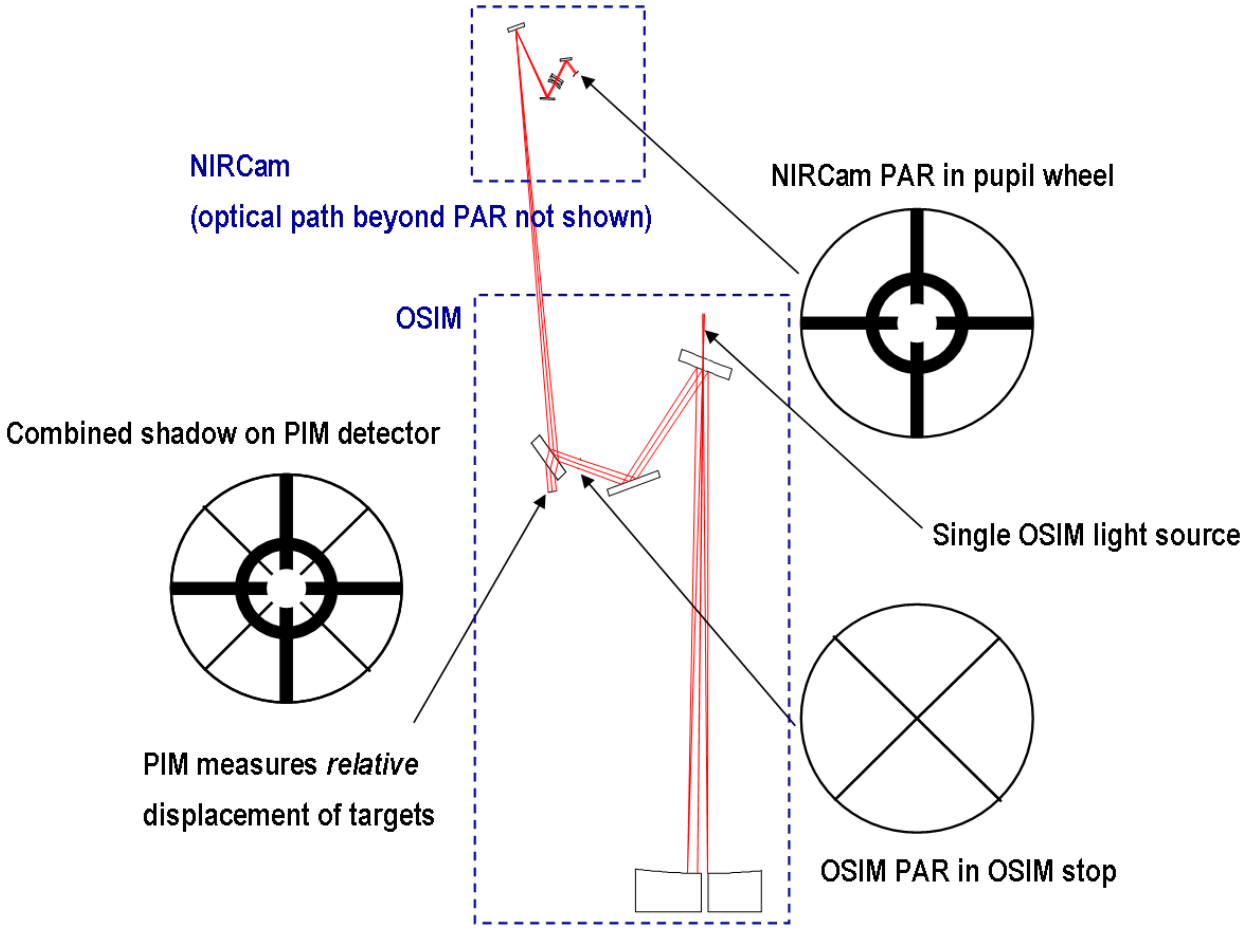

Figure 6. Optical layout of the pupil alignment reference (PAR) measurement approach for the JWST science instruments using the OSIM. The instrument shown in this example is the NIRCam (fiducials shown are only notional and do not represent the final design).

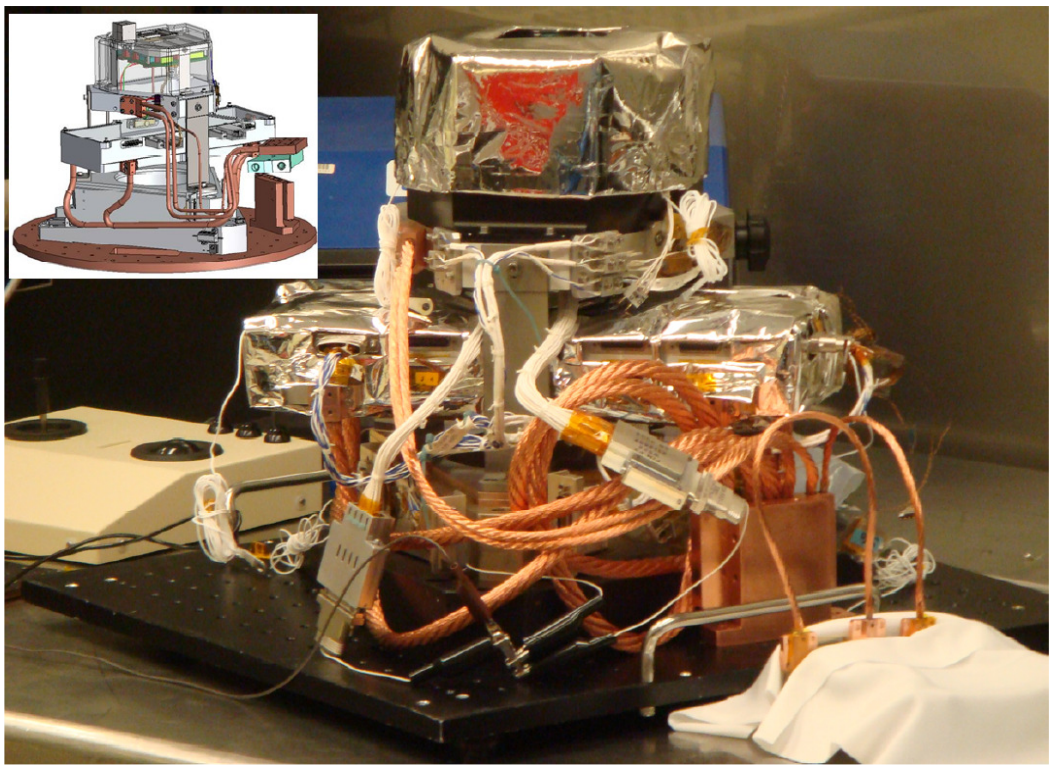

Figure 7. Pupil imaging module (PIM) preparing to undergo cryogenic vacuum testing. The PIM detector aperture is visible at the top part of the photograph. A computer aided design representation of the PIM is shown in the upper left.

Originally the PAR measurement technique used diffusely reflective PARs. But ray tracing analyses indicated the PAR fiducials would be very difficult to detect and measure due to poor image quality at the PIM detector. The primary cause of the poor image quality was determined to be due to the design residual aberrations of the instruments' front-end optics. The primary aberration causing the poor performance was astigmatism. This causes a behavior that the JWST Project has called "pupil wander" because the science instrument entrance pupils move, or wander, with field position[9]. All of the JWST instruments exhibit this phenomenon to varying degrees.

To solve the problem caused by astigmatism in the pupil images we changed the design of the PARs to be specularly reflective instead of diffusely reflective. This made them slightly more difficult to fabricate but improved the PAR image quality significantly. Due to this change, the images that are created at the PIM detector are not classical images but rather are shadows and the detector captures those shadows in a near-field diffraction regime. This generates near-field diffraction ringing at the shadows from the fiducial edges or obstructions in the beam. As long as the PIM detector is located in the general vicinity of the projected image, the ringing does not significantly affect the measurement accuracy. Figure 8 shows near-field diffraction modeling of the PAR measurement technique in each of the five channels where the measurement will be made. Note that in the figure, the images have been scaled so that the images returned by the PARs are all displayed with the same diameter. The fiducial images in the simulation that resemble a ladder are the OSIM PAR fiducials and they can be used to compare the image scales between the various images. The same OSIM PAR is used to generate each image. The lines, circles and crosshairs in the images are the patterns generated by the science instrument fiducials. Near-field diffraction ringing can clearly be seen in the simulations, particularly in the case of the FGS-Guider.

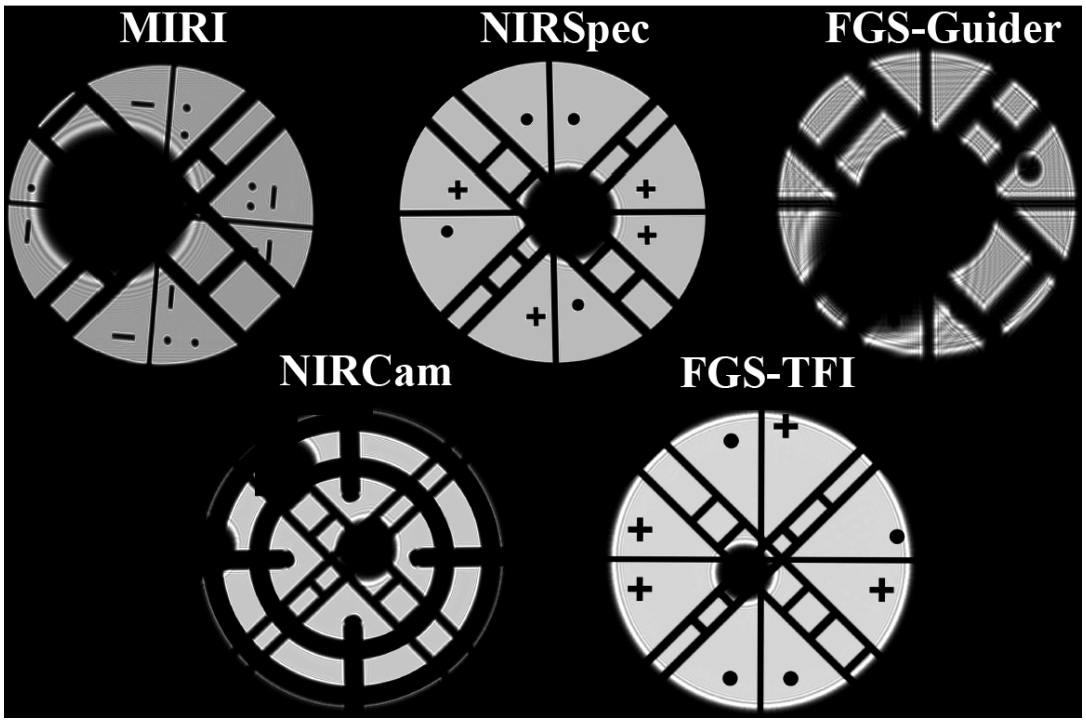

Figure 8. Near-field diffraction simulations of the PAR measurement technique. The images have been scaled so that the images returned by the PARs are all displayed with the same diameter. The fiducial images in the simulation that resemble a ladder are the OSIM PAR fiducials and they can be used to compare the image scales between the various images. The same OSIM PAR is used to generate each image. The lines, circles and crosshairs in the images are the patterns generated by the science instrument fiducials.

3.3 Pupil imaging

In addition to the baseline pupil measurement approach using the PARs, during the ISIM Element testing we will also be using pupil imaging functionality that exists in two of the science instruments to crosscheck the baseline PAR pupil measurements at three field points. The MIRI imager has an alignment lens located in its filter wheel that can be rotated into place to generate an extremely out-of-focus PSF image at the MIRI imager detector plane that resembles the system pupil.[9] And in both of the short wavelength NIRCam A and B channels there are pupil imaging lenses, recently changed for the flight model from a multi-element lens to a singlet, that can be rotated into the optical path on their own dedicated mechanisms to generate images of the NIRCam exit pupils at the NIRCam short wavelength detectors.[11,12]

We will use both of these modes in the NIRCam and MIRI to record images of the OSIM PAR fiducials. Then the fiducial image locations will be compared to the NIRCam and MIRI pupil fiducial images to measure the NIRCam and MIRI pupil alignment using the same analysis procedure as we described in Section 3.2 for the PAR measurements. The fiducials used in this technique, however, will not be the NIRCam or MIRI PAR fiducials.

In NIRCam there are self-illuminated pinholes located in the back of the NIRCam pupil wheels in both of the two NIRCam modules that can be rotated into place. These pinholes are calibrated in a fashion similar to the NIRCam PAR fiducials so that the relationship between the pinholes and the NIRCam science aperture stops are known. The mechanical features that hold the self-illuminated pinholes are opaque. This requires that the NIRCam pupil alignment measurements that use the pupil alignment lens have to be completed by taking images of the OSIM PAR and the NIRCam pinholes with different exposures. The NIRCam detector coordinate system then serves as the common reference between the two images so that the pupil alignment can be measured. Just like the PAR approach, this pupil measurement technique allows us to measure the three key pupil degrees-of-freedom: lateral motion up and down,

Figure 9. Near-field diffraction simulation of the NIRCam pupil imaging lens performance when observing the OSIM PAR.

lateral motion side-to-side and rotation. Figure 9 shows a near-field diffraction modeling prediction of how well the new NIRCam pupil imaging lens singlet will be able to image the OSIM PAR fiducials on the NIRCam short wavelength detectors.

In MIRI there is a diaphragm mounted to the alignment lens which contains fiducials that are calibrated in the same manner as the MIRI PAR fiducials, providing a known relationship between the diaphragm fiducials and the MIRI science apertures. The MIRI alignment lens diaphragm allows most of the OSIM beam through, so a single image recorded on the MIRI imager detector provides enough information to measure the same key pupil degrees-of-freedom that we measure with the PARs and the NIRCam pupil imaging lenses. Two separate images are not required.

Although we can only measure pupil alignment at three field points using the pupil imaging capability in MIRI and NIRCam, we believe it is an important crosscheck to complete. Since the instrument fiducials will be different than what we use during the PAR measurements, we will have the opportunity to discover instrument calibration errors or inconsistencies. In addition, pupil imaging is the only technique available for measuring pupil alignment during the full-up observatory testing that will occur in Chamber A at the Johnson Space Center. By being able to directly compare the PAR-based measurements and the pupil imaging measurements during the ISIM Element testing, we will reduce the risk at the observatory level of misunderstanding how the NIRCam and MIRI pupil alignment measurements relate to the global pupil alignment measurements completed at the ISIM level.

3.4 Pseudo non-redundant mask

Although the NIRCam and MIRI pupil imaging modes provide insight into the shape and relative amplitude of their respective instruments' exit pupil functions, the very introduction of the lenses that allow the observations of those pupils changes what is recorded by the instrument detectors. Those effects need to be calibrated out in order to have accurate pupil function information for phase retrieval as described in Section 2.3. In addition, the other JWST instruments do not have pupil imaging capabilities at all and so we had to develop a measurement approach that would allow us to measure the instruments' exit pupil distortion and amplitude.

Unfortunately our baseline pupil characterization approach using the PARs cannot access the instrument exit pupils to measure them. Light only travels into the instruments as far as the PARs, which are located close to the instruments'

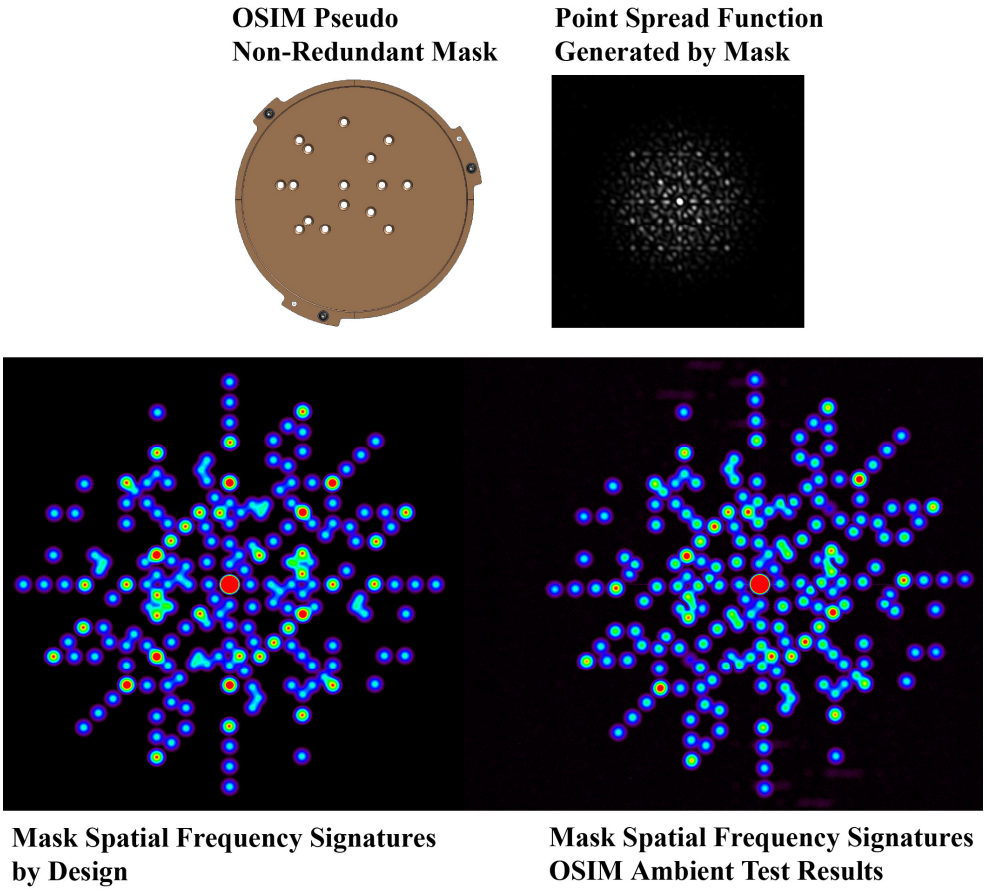

Figure 8. Upper left: solid model design representation of the OSIM pseudo non-redundant mask. Upper right: the optical point spread function generated by the OSIM pseudo non-redundant mask. Lower left: the spatial frequency signatures generated by the mask after Fourier transforming the point spread function. Lower right: the spatial frequency signatures generated by the mask during OSIM ambient temperature testing with an instrument surrogate detector.

aperture stops, and then it gets reflected back towards the OSIM. So to do this important instrument exit pupil characterization for phase retrieval, we have developed a special OSIM aperture mask called the pseudo non-redundant mask.

The pseudo non-redundant mask is a new type mask that contains 16 holes positioned in a particular way so that when it is introduced into the OSIM optical path, it generates a point spread function in the instrument detector planes with specific spatial frequency signatures. The holes are arranged so that the apparent hole-to-hole distances as they occur in the instrument exit pupils can be determined unambiguously by analyzing the Fourier transform of the recorded point spread function. In addition, the spatial frequency signature peaks can be analyzed to determine the relative pupil amplitude at the locations in the pupil that the holes sampled. This will allow us to not only calibrate out the MIRI alignment lens and the NIRCam pupil imaging lens' affect on the MIRI and NIRCam exit pupil images but it will also provide exit pupil characterization for those instruments that do not have pupil imaging channels (NIRSpec, FGS-Guider and FGS-TFI).

Figure 8 shows the OSIM pseudo non-redundant mask, the point spread function it produces and the two-dimensional spatial frequency signatures it generates in spatial frequency space. In the lower right hand corner of Figure 8 actual test results are shown from ambient testing of the OSIM using a surrogate detector plane in place of the science instruments. Performance matches the design intent very closely.

3.5 Aperture edge identification mask

Although we will be able to determine the JWST instrument pupil alignment very accurately using the PAR measurement technique and crosscheck those measurements at three field points using the NIRCam and MIRI pupil imaging modes, we decided that the observatory performance degradation caused by rogue path stray light is so great that we needed another pupil measurement approach to ensure that the path is indeed closed. To do this we designed an additional OSIM mask for testing at the ISIM Element level.

The mask we designed to do this measurement utilizes some of the same Fourier optics concepts as the pseudo non-redundant mask but its only purpose is to locate the edges of the science instrument projected entrance pupils at the OTE FSM mask location. And the only pupil edges it is designed to find are those that are closest to the rogue path.

As shown in Figure 9, the aperture edge identification mask contains 8 holes. Just like all the OSIM aperture masks the mask is mounted to a mechanism that can translate the mask laterally under cryogenic vacuum conditions. When testing with the mask commences, the aperture mask will be positioned away from the nominal OSIM pupil edge to ensure that light from all 8 holes can make it through the instrument under test to the instrument's detector plane. This position will be informed by the PAR pupil measurement results which will be acquired before this test is started. After an initial point spread function is acquired from the science instrument's detector, the mask will be translated laterally to move the four probe holes toward the expected edge of the science instrument's projected entrance pupil, the edge that could let in the rogue path. After each mask step, the instrument's point spread function will be recorded. This process will be repeated until the end of the OSIM lateral translation range is reached or until no light can be sensed falling on the instrument detector. The mask will then be moved back to the initial starting position and the process repeated in a slightly different scan direction. Multiple scans are planned for each instrument so that the mask's probe holes intersect the science instrument projected entrance pupil edges in multiple places.

Finding the projected entrance pupil edges of the science instruments will be done by analyzing the point spread function images that are acquired during the mask scans. The point spread functions will be Fourier transformed and then the spatial frequency signatures inspected to see which signatures exist. Due to the locations of the holes designed into the mask, each of the 4 probe holes will generate unique spatial frequency signatures with the reference holes that can not be

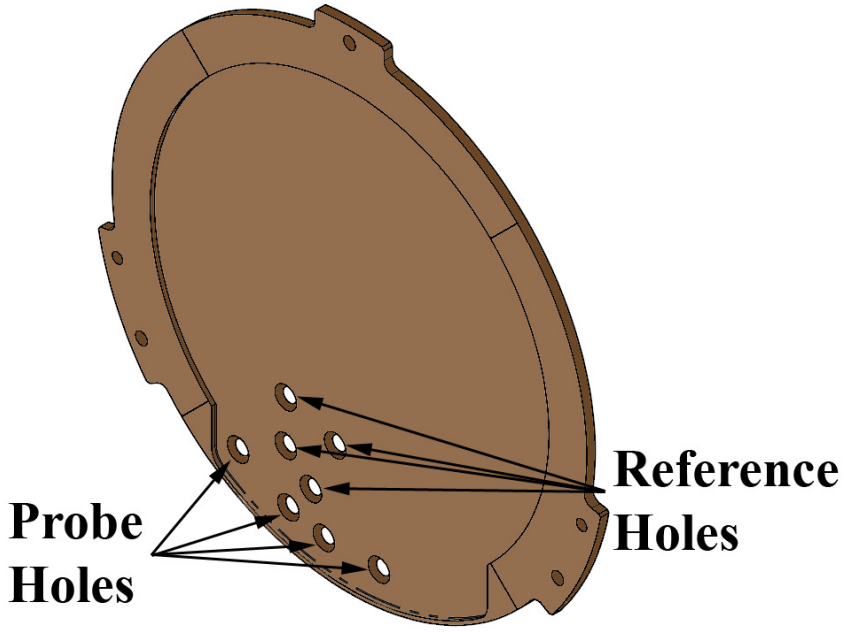

Figure 9. The OSIM aperture mask used to locate the edges of the science instrument projected entrance pupils in the vicinity of the JWST rogue path.

confused with any of the other probe holes. When those spatial frequency signatures disappear, we will know exactly which one of the probe holes is being blocked by the internal aperture stop of the science instrument being tested. Then, based on the OSIM mask calibration data, we will know where in the projected entrance pupil space one point of the entrance pupil edge is located. By finding multiple points on the edges of the projected entrance pupils we will be able to use our knowledge of the internal aperture stop shape to find a best fit through all the measurement points so that the entire edge of the pupil that is close to the rogue path can be determined.

An additional component of the test data analysis will be the calculation of the science instrument relative responses with OSIM mask position. From this we should get corroborating evidence about how many holes are being blocked, consistent with the spatial frequency analysis. The radiometric information will not be able to tell us which holes are being blocked but it will provide additional insight into the spatial frequency analysis results if something unexpected is observed due to detector noise, stray light or thermal background noise.

4. SUMMARY AND LESSONS LEARNED

Our development work on the James Webb Space Telescope has identified key pupil alignment issues for the observatory that we believe will also be important to the large, deployable space telescopes that follow. For JWST, good pupil alignment is key to the primary science goal of the mission to observe the very first stars and galaxies to form in the Universe more than 13 billion years ago. If the JWST science instrument projected entrance pupils are misaligned with respect to the OTE exit pupil, instrument optical sensitivity will be degraded; coronagraphic observations and the study of extra-solar planets will be compromised; and entire observing campaigns may become impossible if rogue path stray light reaches the instrument pick-off mirrors. But JWST does not only require accurate alignment of the pupils, knowledge of the science instrument exit pupil characteristics is also important to the success of the mission. The use of phase retrieval in the on-orbit construction of the observatory necessitates the availability of accurate exit pupil shape and amplitude information.

To ensure that JWST will perform satisfactorily on-orbit, we have developed four different types of pupil measurement tests that will be conducted during the ISIM Element cryogenic vacuum test campaign to determine pupil alignment and pupil characteristics. Our primary test of the three key pupil alignment degrees of freedom, lateral motion side-to-side and up-and-down, and pupil roll, is conducted using pupil alignment references in each of the JWST science instruments and a special detector and beam splitter in our optical ground support equipment. We also have the ability to crosscheck those results at three field points by conducting a second type of test that uses existing pupil imaging capabilities in two of the JWST science instruments. In addition, due to the severe impact rogue path stray light could have on the JWST observing program, we have developed a third test to check pupil alignment that will specifically check for the location of the science instrument projected pupils in the vicinity of the rogue path. And finally, to provide science instrument exit pupil characterization for our phase retrieval algorithms, we have developed a new kind of mask for a fourth type of pupil testing that will provide exit pupil distortion and relative pupil amplitude calibration.

Based on what we have learned thus far on the JWST Project, we believe that there are two key capabilities that future mission designers should consider including in the instruments of large, deployable space telescopes. The first is an on-orbit pupil alignment capability. NIRCam has this capability but none of the other JWST science instruments do. We believe the benefits, both to on-orbit operations and to the ground verification program, far outweigh the added expense of such a capability. It provides significant mitigation against certain stray light paths, which are hard to test for on the ground, and it allows you to expect tighter tolerances for pupil alignment so that coronagraphs can be designed with more sensitivity and aperture stops can better control stray light without risking vignetting.

The second capability we recommend including in the design of future instruments for large, deployable space telescopes is the ability for the instruments to characterize their own exit pupils. This can be done using a pseudo non-redundant mask located in the instruments' pupil wheels or with some type of pupil imaging lens similar to what the NIRCam and MIRI have. We believe that some method for crosschecking the pupil assumptions that are used as inputs into the phase retrieval codes used to build the telescopes on-orbit eliminates a significant amount of risk from the mission and also significantly reduces the cost of the ground test campaign.

REFERENCES

[1] Greenhouse, M. A., Sullivan, P. C., Boyce, L. A., Glazer, S. D., Johnson, E. L., McCloskey, J. C. and Voyton, M. F., "The James Webb Space Telescope integrated science instrument module," Proc. SPIE 5487, 754-764 (2004).

[2] Horner, S., Rieke, M. and the NIRCam team, "The Near Infrared Camera (NIRCam) for the James Webb Space Telescope (JWST)," Proc. SPIE 5487, 628-634 (2004).

[3] Posselt, W., Holata, W., Kulinyak, E., Kling, G. and Kutscheid, T., "NIRSpec: near-infrared spectrograph for the JWST," Proc. SPIE 5487, 688-697 (2004).

[4] Wright, G. S., et al., "The JWST MIRI instrument concept," Proc. SPIE 5487, 653-663 (2004).

[5] Rowlands, N., et al., "The JWST fine guidance sensor," Proc. SPIE 5487, 664-675 (2004).

[6] Rowlands, N., Evans, C., Greenberg, E., Gregory, P., Scott, A., Thibault, S., Poirer, M., Doyon, R., Hutchings, J. and Alexander, R., "Tunable filters for JWST Fine Guidance Sensor," Proc. SPIE 5487, 676-687 (2004).

[7] Bos, B. J., Davila, P. S., Jurotich, M., Hobbs, G., Lightsey, P., Contreras, J. and Whitman, T., "The James Webb Space Telescope instrument suite layout: optical system engineering considerations for a large, deployable space telescope," Proc. SPIE 5487, 734-745 (2004).

[8] Sullivan, J., et al., "Manufacturing and Integration Status of the JWST OSIM Optical Simulator," Proc. of SPIE 7731, 77313V (2010).

[9] Bos, B. J., Kubalak, D. A., Antonille, S. R., Ohl, R. G., Hagopian, J. G., Davila, P. S., Sullivan, J., Sánchez, M., Sabatke, D., Woodruff, R. A., te Plate, M., Evans, C., Isbrucker, V., Somerstein, S., Wells, M. and Ronayette, S., "Cryogenic pupil alignment test architecture for the James Webb Space Telescope integrated science instrument module," Proc. SPIE 7010, 70103C (2008).

[10] Sabelhaus, P., Geithner, P. and Diaz, C., "Cryogenic Optical Thermal-Vacuum Testing of the James Webb Space Telescope (JWST)," Aerospace Conf., 2007 IEEE, 1-6 (2007).

[11] Clark, C. S. and Jamieson, T., "NIRCam pupil imaging lens mechanism and optical design," Proc. SPIE 5904, 59040C-1 (2005).

[12] Dean, B. H., Bos, B. J., "Wave-Optics Analysis of Pupil Imaging," Proc. SPIE 6265, 62653H-1 (2006).

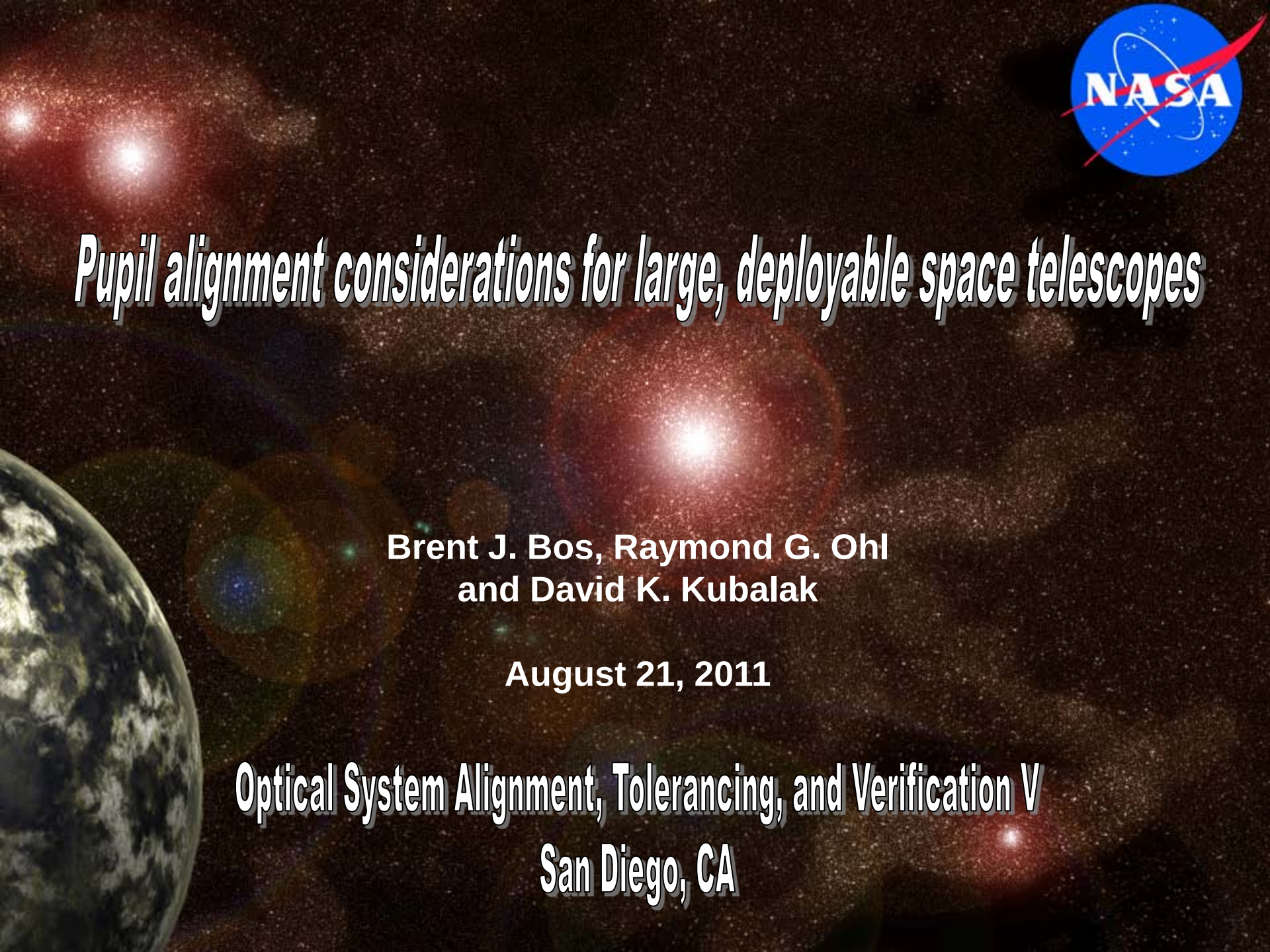

Pupil alignment considerations for large, deployable space telescopes

Brent J. Bos, Raymond G. Ohl
and David K. Kubalak

August 21, 2011

Optical System Alignment, Tolerancing, and Verification V
San Diego, CA

James Webb Space Telescope (JWST)

- JWST is the “follow-on” mission to the Hubble Space Telescope (HST)
  - Wavelength overlap with HST but coverage is not the same.
- First space telescope to be “built” on-orbit – too large to be launched already assembled.
- Mission concept formulated in 1995, 2018 launch date.

Primary Science Goal for JWST is to observe the Universe when it first began to emit light, approximately 200 Million years after the Big Bang

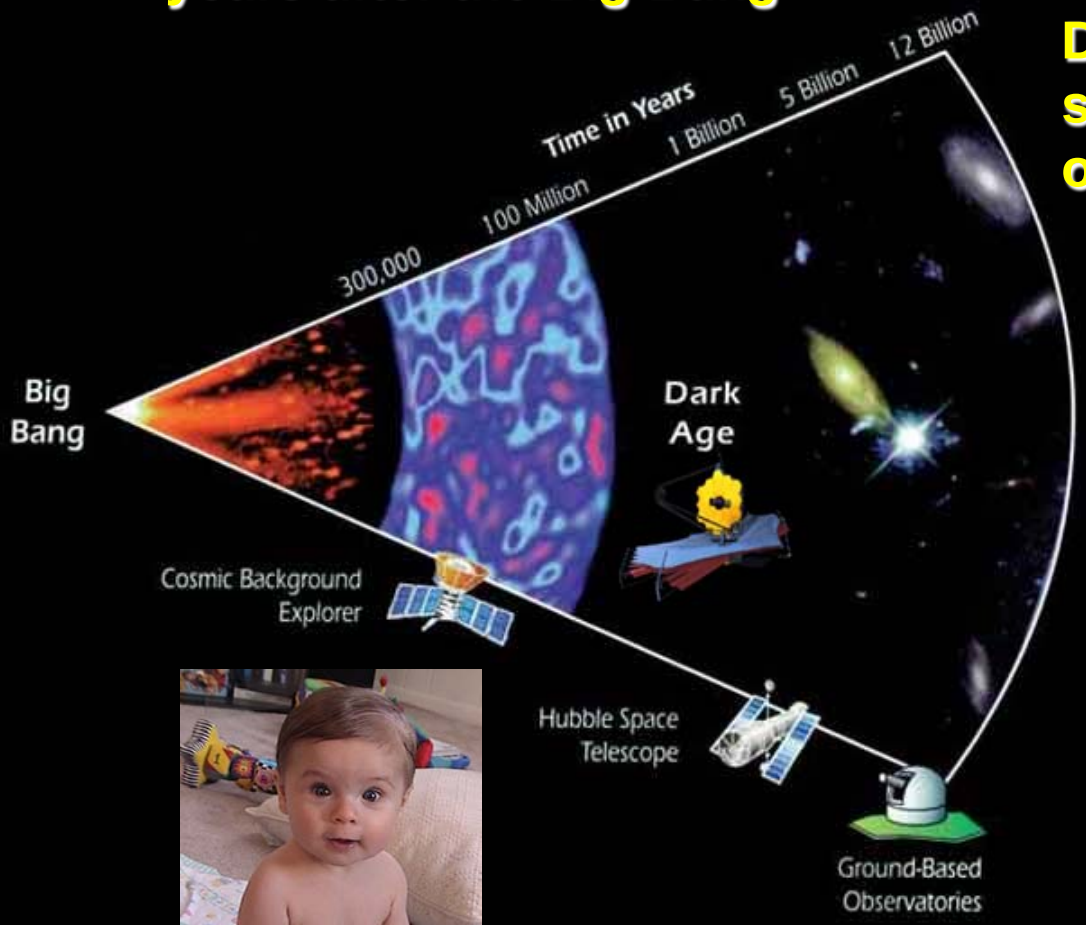

Distant astronomical sources have redshifts (z) of 10 or more

$$\lambda_{motion} = \lambda_{rest} + z\,\lambda_{rest}$$

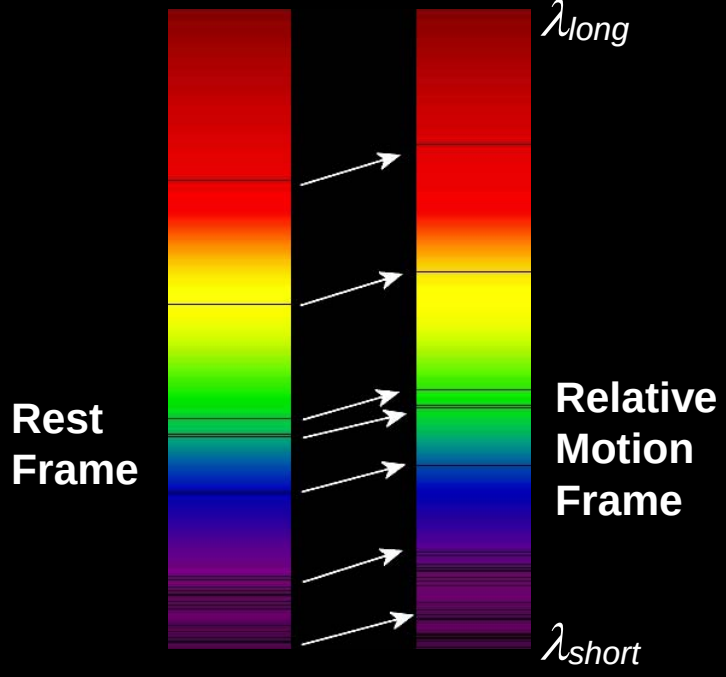

Due to the Doppler shift of the emitted light, looking back that far in time requires the ability to make infrared observations

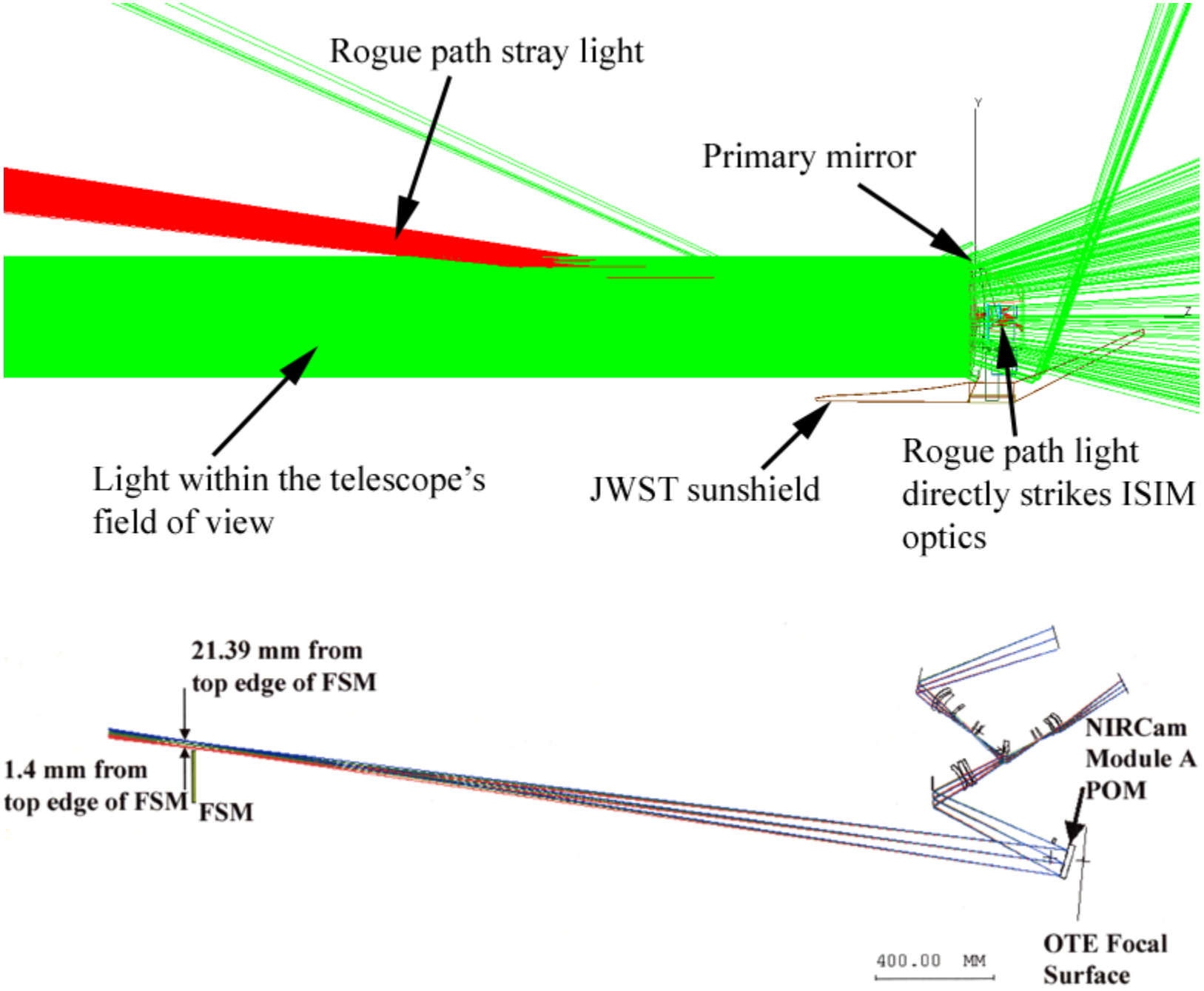
Rogue path stray light
Primary mirror
Light within the telescope's field of view
JWST sunshield
Rogue path light directly strikes ISIM optics
21.39 mm from top edge of FSM
1.4 mm from top edge of FSM
FSM
NIRCam Module A POM
OTE Focal Surface
400.00 MM

Rogue Path Mitigation

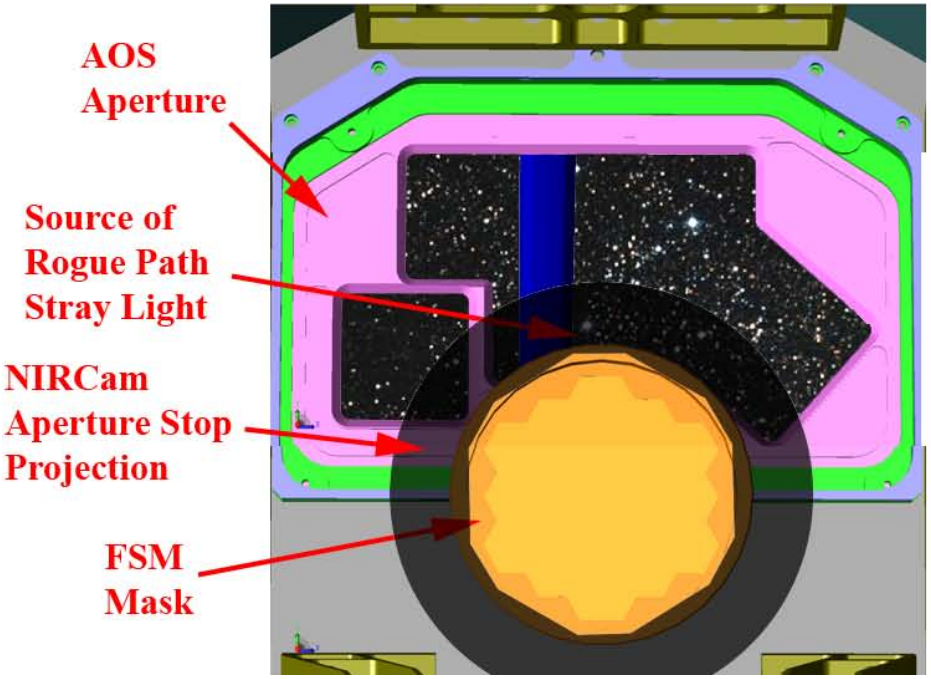

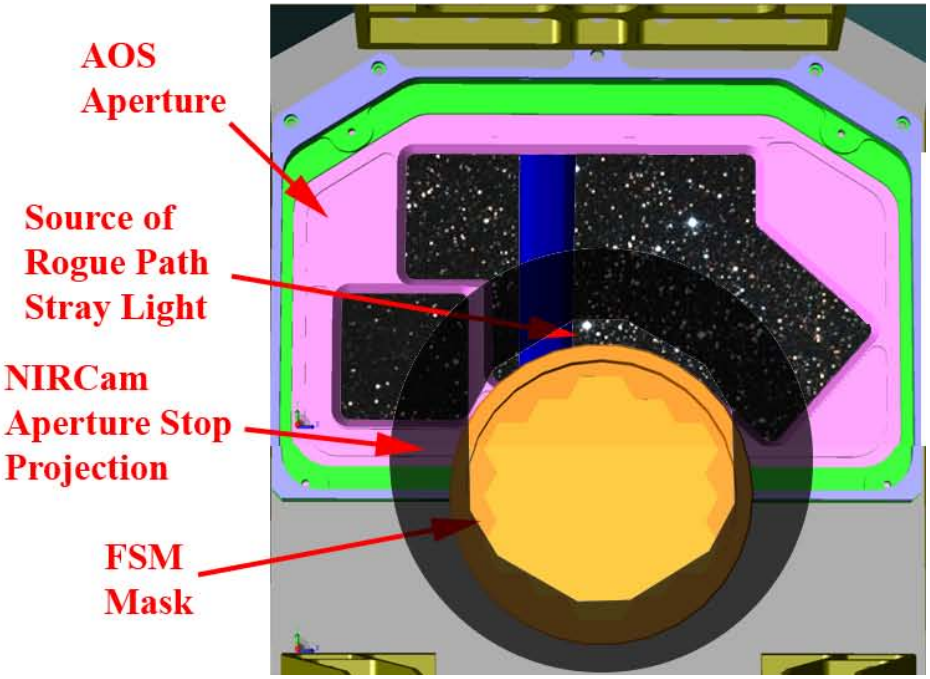

Pupil Alignment Measurement Trades

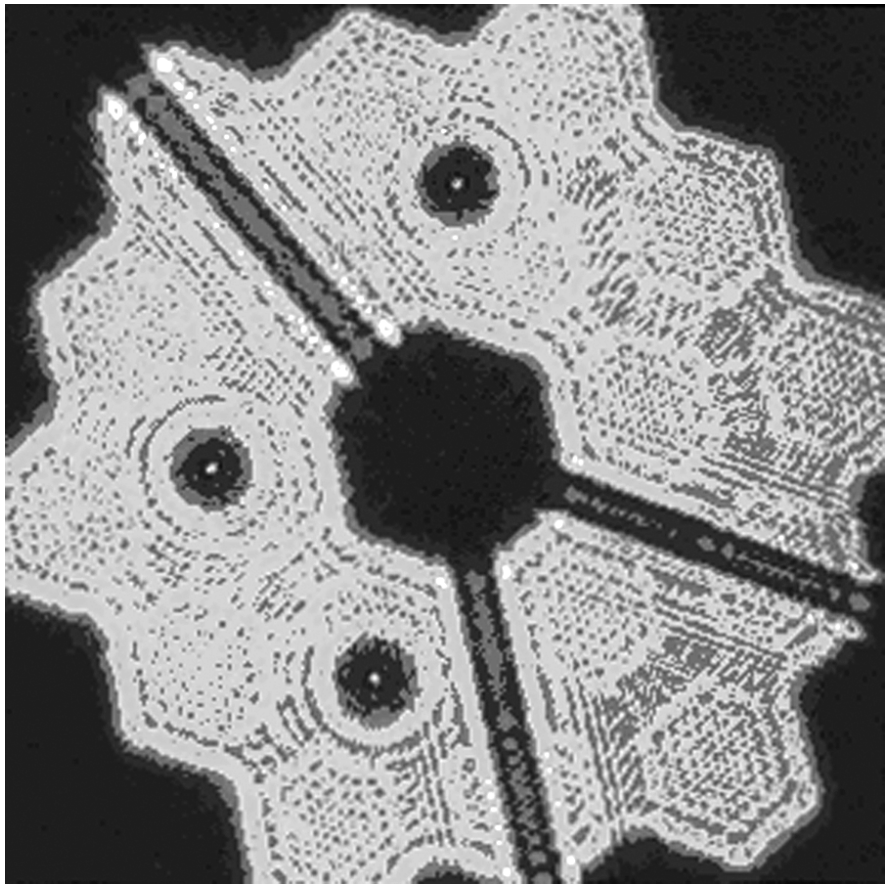

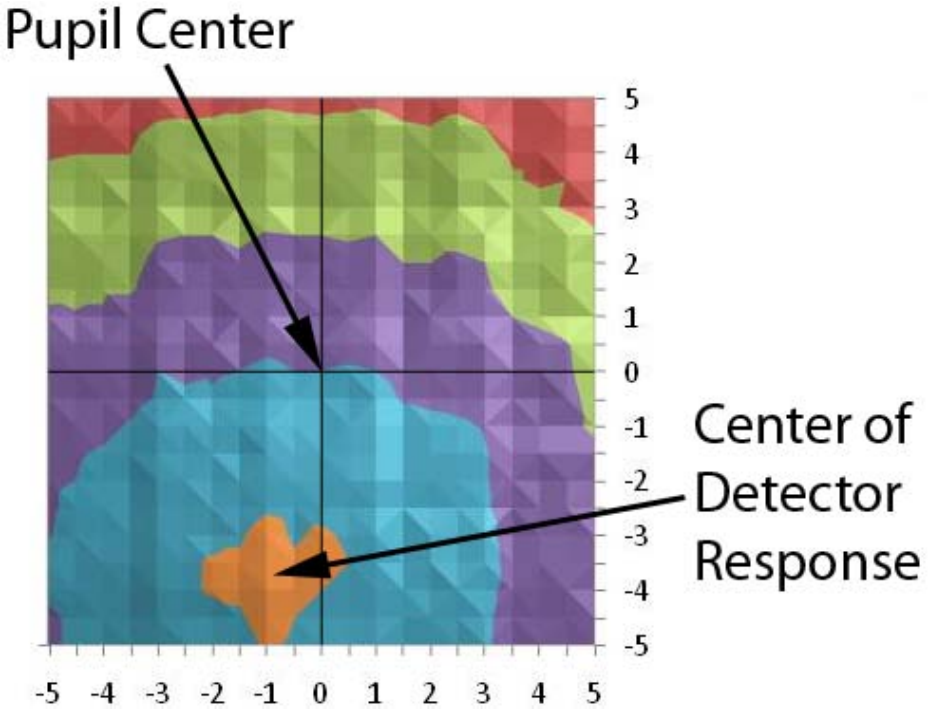

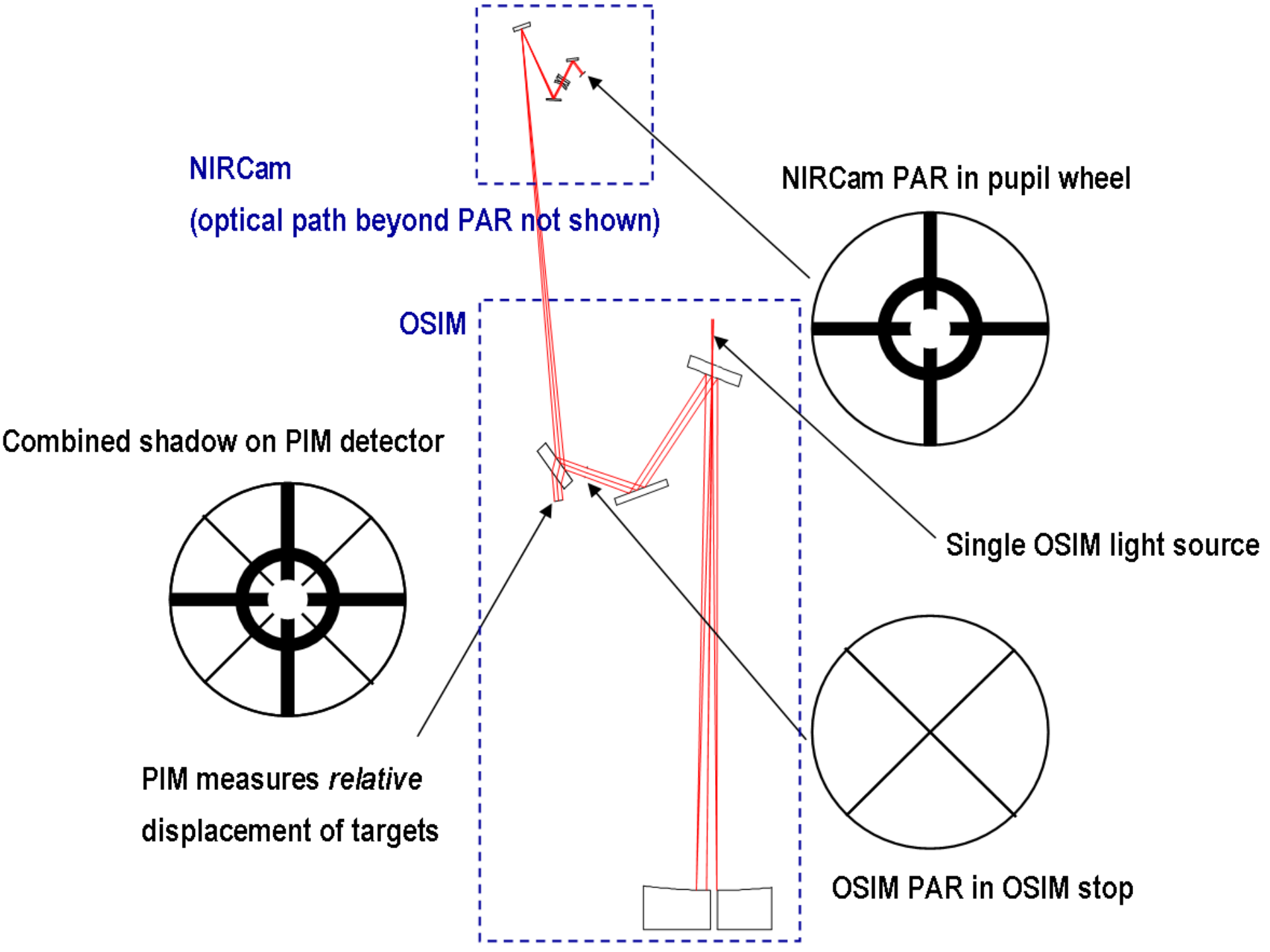
NIRCam
(optical path beyond PAR not shown)
NIRCam PAR in pupil wheel
OSIM
Combined shadow on PIM detector
Single OSIM light source
PIM measures *relative*
displacement of targets
OSIM PAR in OSIM stop

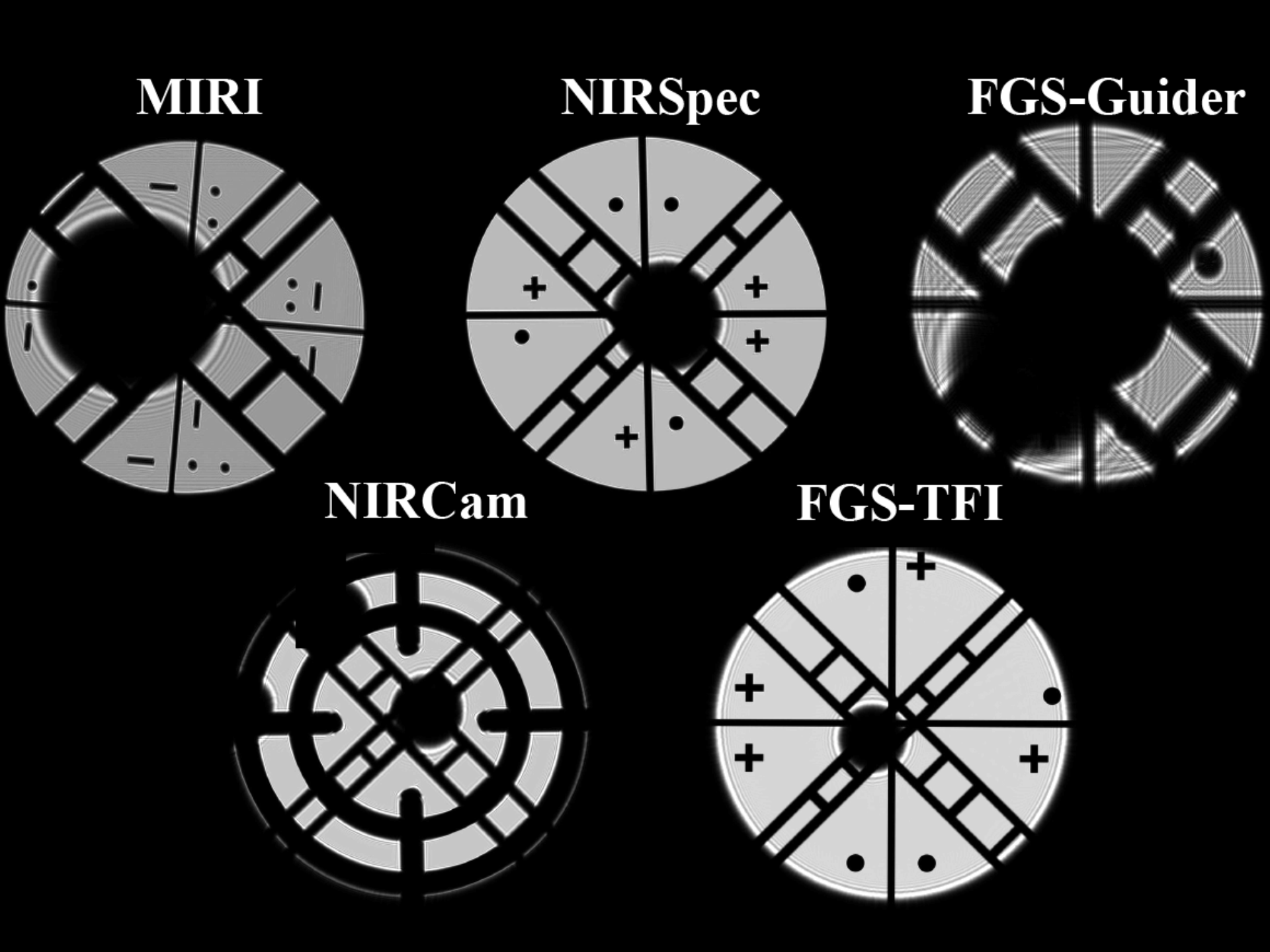
MIRI
NIRSpec
FGS-Guider
NIRCam
FGS-TFI

Pupil Measurement Crosschecks

Pupil Distortion and Amplitude Measurement

OSIM Pseudo
Non-Redundant Mask

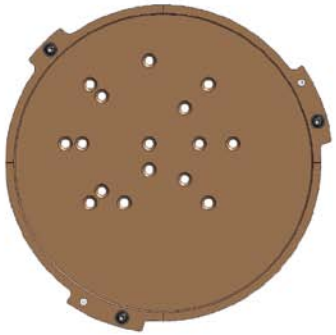

Point Spread Function
Generated by Mask

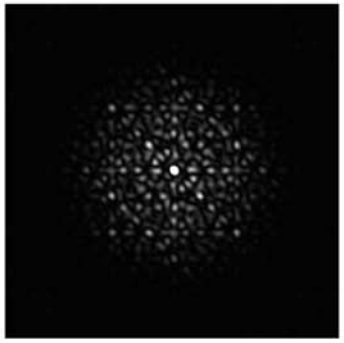

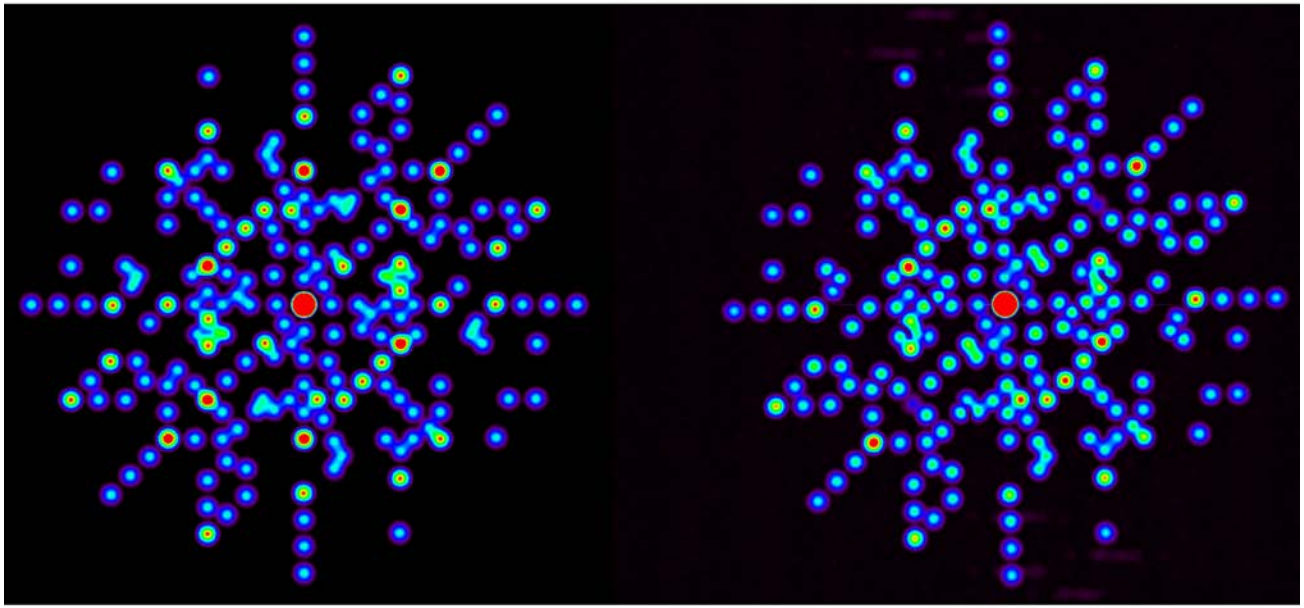

Mask Spatial Frequency Signatures
by Design

Mask Spatial Frequency Signatures
OSIM Ambient Test Results

Rogue Path Mask

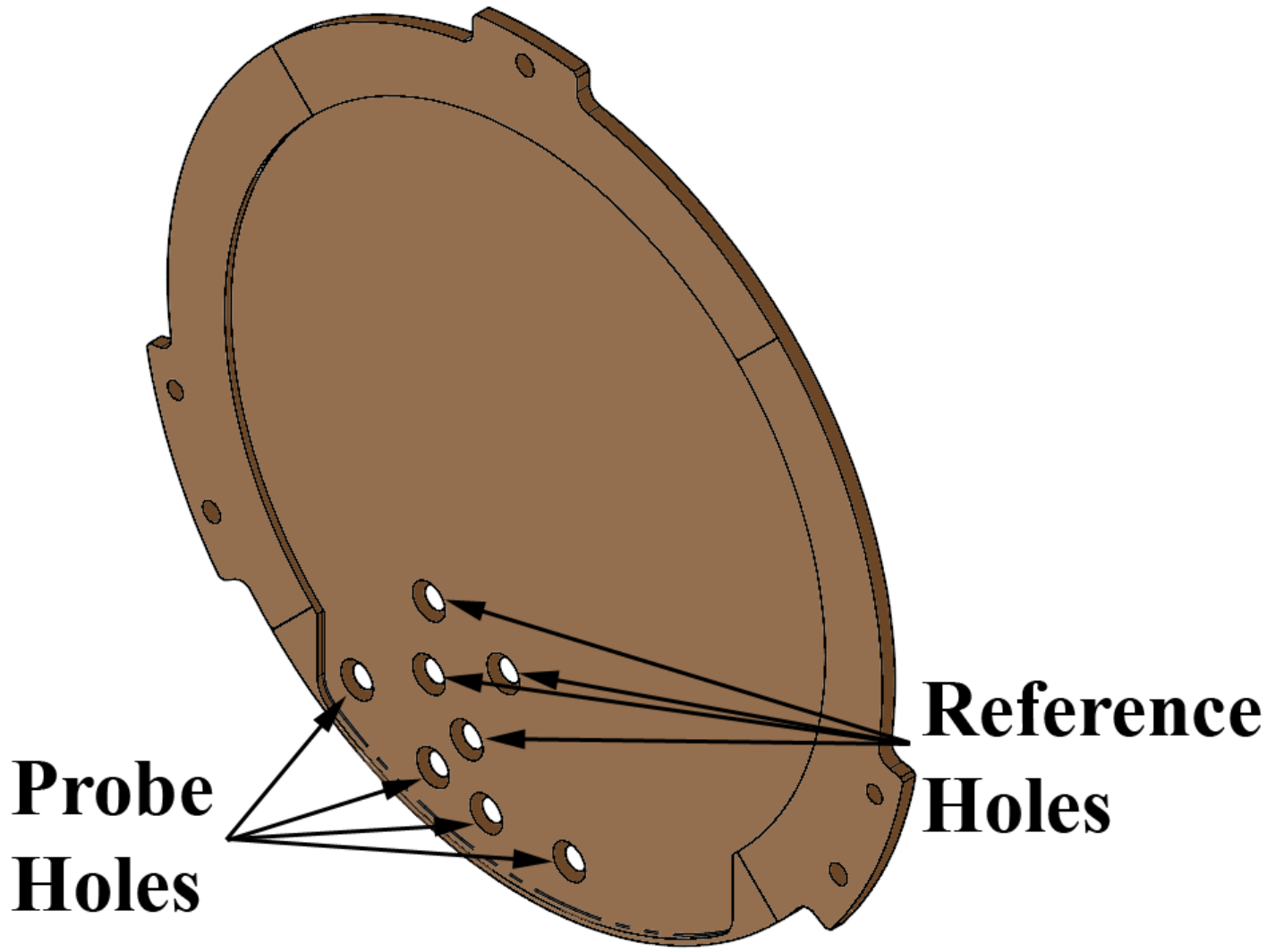

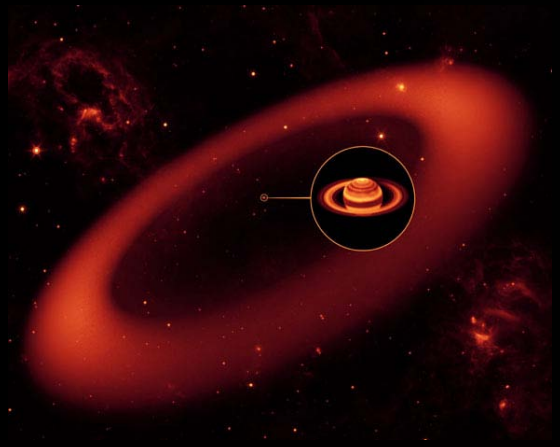
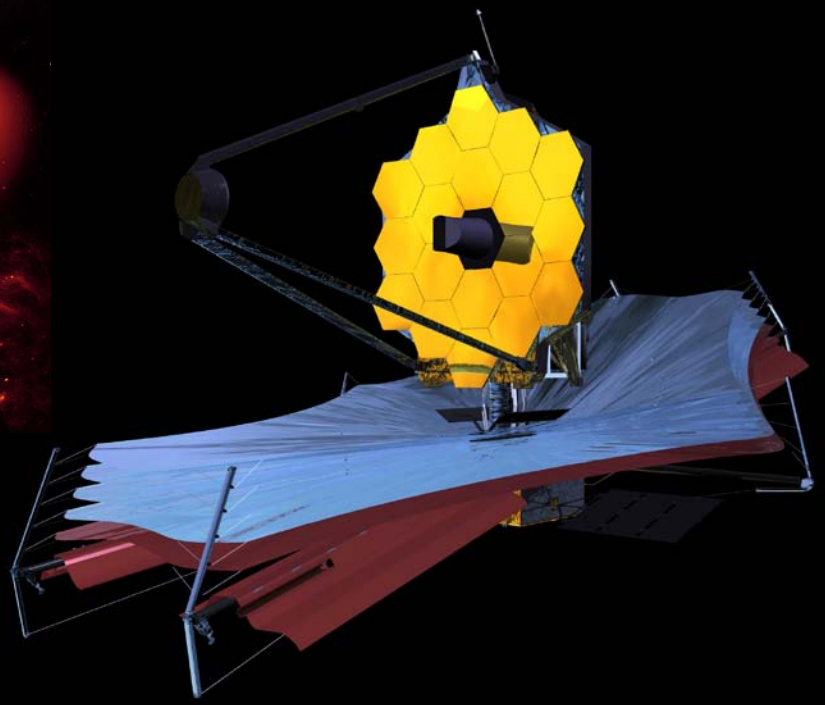


Summary

- Pupil alignment verification and pupil characterization are critical to the success of JWST
  - Vignetting must be avoided to maintain sensitivity.
  - Coronagraphy requires accurate pupil alignment.
  - Gross pupil misalignment will open a serious stray light path.
  - Wavefront sensing and control needs accurate pupil information.
- We have developed a robust pupil verification and characterization test program for the key observatory pupil alignment test
  - Pupil alignment references (PAR)
  - Pupil imaging
  - Special optical ground support equipment masks.